Energy-Efficient, Secure, and Spectrum-Aware Ultra-Low Power Internet-of-Things System Infrastructure for Precision Agriculture

Ankit Mittal, *Graduate Student Member, IEEE*, Ziyue Xu, *Graduate Student Member, IEEE*, and Aatmesh Shrivastava, *Senior Member, IEEE*

***Abstract*—This article presents a robust, energy-efficient, and spectrum-aware infrastructure to support the Internet-of-Things (IoT) system deployed in precision agriculture, aiming to reduce power consumption to a level feasible for sustained operation using harvested energy alone. We present a system modeling-based approach to identify key optimizations, which are subsequently translated into a more feasible ultra-low power (ULP) IoT system implementation. Measurement results for ULP infrastructure components, including a ULP received signal strength detector and wake-up radio, implemented in a 65-nm CMOS technology, demonstrate power consumption in the range of a few nano-watts. In addition, we propose a *lightweight* energy-detection-based countermeasure against energy depletion attacks within IoT networks. We also suggest strategies for IoT sensor nodes to coexist within increasingly congested device networks while opportunistically enhancing their energy systems to potentially achieve self-powered IoT operation. Finally, we conduct a detailed analysis of power consumption in an IoT sensor deployed for sensing and monitoring, evaluating the feasibility of different energy systems, such as battery-based and energy harvesting solutions.**

***Index Terms*—Beamforming, energy harvesting, hardware security, Internet of Things (IoT), jamming attacks, precision agriculture, received signal strength indicator (RSSI), spectrum sensing, system modeling, wake-up radio (WuRx).**

I. Introduction

In recent years, the agriculture sector has experienced a remarkable transformation with the widespread deployment of Internet of Things (IoTs) sensors tailored for precision agriculture and smart farming applications [1], [2], [3], [4], [5], [6], [7]. Fig. 1 illustrates one such IoT network implemented for sensing and monitoring activities in an agricultural setting. These IoT sensors are crucial in gathering data on vital parameters such as soil conditions and ambient factors essential for precision farming practices [1], [8]. Subsequently, this information undergoes processing before being transmitted to gateway devices for further analysis and appropriate actions. A majority of these IoT sensors have to operate in a resource-constrained environment where the energy system to support key communication and computation capabilities is expected to either operate from harvested energy [9] or sustain several years of battery life.

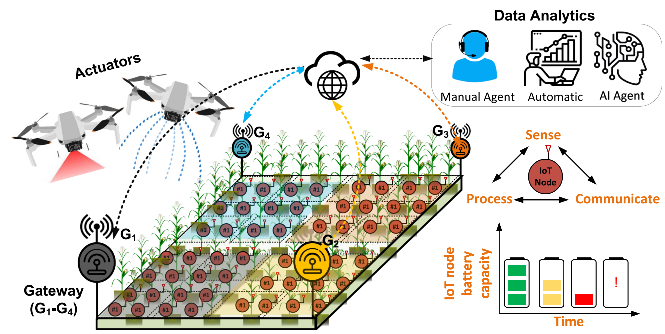

Fig. 1. IoT sensor system is deployed for precision agriculture. IoT node drops out of the network when its limited energy system is exhausted.

Despite technological advancements in precision agriculture [1], [2], [3], significant challenges including security, cost, reliability, and quality of service still impede the scalability and integration of these systems within the IoT framework. Comprehensive discussions in studies [10], [11], [12], [13], and [14] present current agricultural technologies and explore persistent issues in the realm of IoT and precision agriculture.

All-time connectivity which requires these sensors to remain connected in the network for the exchange of useful information, comes at the expense of power hungry radios. The integration of these innovative agricultural technologies also brings to the forefront concerns about data security [10], [11]. In addition, these systems possess limited security capabilities compared to more conventional computing systems and are prone to attacks where available resources can be further exhausted to launch new kinds of security attacks [3], [6], [15], [16]. Moreover, expanding the scope of this IoT network to establish a comprehensive sensing and monitoring system leads to an increased congestion within the shared wireless medium, thereby disrupting network services. This congestion renders spectrum unavailable for communication, forcing IoT nodes to remain in active mode and further depleting their limited energy resources. This necessitates a focus on technologies and frameworks designed to

Manuscript received 13 February 2024; revised 13 May 2024; accepted 30 May 2024. The work was supported in part by the National Science Foundation (NSF) under Grant CCSS-2225368 and Grant RINGS-2146754 with funds from OUSD R&E, NIST, and industry partners as specified in the Resilient & Intelligent NextG Systems (RINGS) program. This article was recommended by Associate Editor F. Rivet. *(Corresponding author: Ankit Mittal.)*

Ankit Mittal and Aatmesh Shrivastava are with the Department of Electrical and Computer Engineering, Northeastern University, Boston, MA 02115 USA (e-mail: mittal.ank@northeastern.edu; aatmesh@ece.neu.edu).

Ziyue Xu is with the Skyworks Solutions Inc., Andover, MA 01810 USA (e-mail: xu.ziy@northeastern.edu).

Digital Object Identifier 10.1109/TAFE.2024.3409166

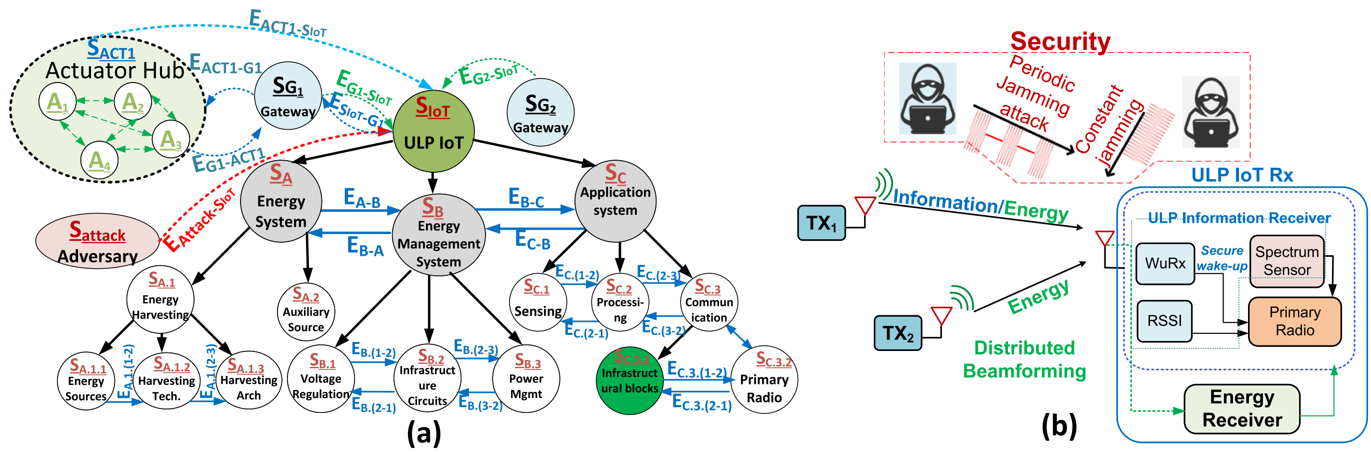

Fig. 2. (a) System graph model identifying key system components and interconnections for holistic optimization of the ULP IoT system. (b) Proposed framework to enhance energy efficiency, security and co-existence within the IoT network.

address spectral congestion in precision agriculture. Alghazzawi et al. [17] presented a congestion management protocol for data transmission in agricultural systems.

Consequently, to extend the lifespan of deployed IoT systems and achieve the "*deploy and forget*" objective, we propose an energy efficient, secure, and spectrum-aware infrastructure for the IoT system. This infrastructure is designed to mitigate existing shortcomings and enhance overall system performance.

We summarize the main contribution as follows.

1) It introduces a generalized system graph depicting an IoT system deployed for precision agriculture and identifies critical optimizations aimed at enhancing the energy efficiency, security, and spectral awareness of the IoT system.
2) It translates these model-based optimizations into a practical IoT sensor system and proposes circuits to implement a robust IoT infrastructure powered by an enhanced energy system, potentially enabling self-powered operations for precision agriculture.
3) In addition, it presents the architecture of the energy receiver and provides simulation results demonstrating the amplification of harvested energy in the system through distributed beamforming.
4) It conducts a comprehensive analysis of the power consumption of the sensor hub, utilizing a practical case study, to assess the viability of energy harvesting as a solution for achieving energy autonomy in sensing and monitoring for precision agriculture.

The rest of this article is organized as follows. In Section II, we present a generalized system model of the ultra-low power (ULP) IoT system, identify key optimizations, and establish a feasible ULP IoT system framework. Section III discusses the design of ULP infrastructural blocks to improve the energy efficiency, security, and spectrum awareness of the information receiver. Section IV presents an energy receiver for the ULP IoT system which can boost the IoT node's energy system. In Section V, we conduct a comprehensive analysis of the power usage of a sensor hub employed for monitoring and sensing tasks. In addition, a practical example has been utilized as a case study to assess the viability of various energy systems. Finally, Section VI concludes this article.

II. System Architecture

In this article, we have applied the generalized system's theory, which has considerably optimized physical [18], and socio-economic systems [19], [20], to model the ULP IoT system deployed for precision agriculture. This approach allows us to efficiently translate theoretical insights into a practical infrastructure tailored to the IoT system's needs.

A. Generalized System Model

In Fig. 2(a), we present the generalized system model for the ULP IoT system. We have limited the system components in our model without compromising the generalized representation to illustrate the systems philosophy [18] applied to ULP IoT system optimizations.

The system model comprises a ULP IoT node (S_{IoT}) which interacts with the gateway devices (S_{G1}, S_{G2}). Relevant physical parameters (soil, water, air, crop quality) are routed, upon request ($E_{G_1-S_{\text{IoT}}}$), to (S_{G1}) through the communication system ($S_{C.3}$) using relevant IoT protocol [1]. (S_{G1}) performs analysis on the gathered data from the multiple IoT sensors. Actuator hub (S_{ACT1}) comprises of in-field stationed or unmanned aerial vehicles (UAV) actuators and performs an appropriate action (irrigation, pest spray, etc.) based on the command received from (S_{G1}). This process of *sensing, communication, processing, and actuation* is modeled by the graph edges ($E_{G_1-S_{\text{IoT}}} \rightarrow E_{C.3.(1-2)} \rightarrow E_{S_{\text{IoT}}-G_1} \rightarrow E_{G_1-\text{ACT}_1} \rightarrow E_{\text{ACT}_1-S_{\text{IoT}}}$).

(S_{IoT}) activates *sleep mode* for its power hungry subsystems particularly primary radio ($S_{C.3.2}$) which otherwise in an *always-on* mode would significantly overload the energy system (S_A) and decrease IoT node's lifetime. Wake-up radio (WuRx), a subsystem of ($S_{C.3.1}$), wakes-up ($S_{C.3.2}$) upon a gateway request. Once it communicates the sensed data, ($S_{C.3.2}$) reenters into *sleep mode* to conserve its limited available energy. Recent PHY/MAC layer attacks, such as energy depletion attack (EDA), target this energy-saving mechanism of (S_{IoT}) forcing frequent

TABLE I
SYSTEM GRAPH MODEL AND PROPOSED OPTIMIZATIONS

Graph Nodes (V)	
System Component	**Proposed System/Model**
Energy System (S_A)	Efficient Rectifier ($S_{A.1}$)
Communication System ($S_{C.3}$)	RSSI, WuRx optimization ($S_{C.3.1}$)
Actuator Hub (S_{ACT1})	-
Gateway Hub (S_{G1}, S_{G2})	-
Network Adversary (S_{attack})	Constant and Deceptive Jammer
Graph Edges (E)	
Gateway-IoT node link ($E_{G_{1,2}} - S_{\mathrm{IoT}}$)	Distributed Beamforming (S_{G_1}, S_{G_2})
Attacker-IoT node link ($E_{\mathrm{attack}} - S_{\mathrm{IoT}}$)	Energy detection-based countermeasure

wake-ups and reducing energy savings in *sleep mode*. The presence of such adversaries (S_{attack}) necessitates lightweight countermeasures that can defend against such attacks ($E_{\mathrm{Attack}-S_{\mathrm{IoT}}}$) while ensuring minimal loading of (S_A). Extensive monitoring of agricultural fields is accomplished through a network of multiple gateway devices that cater to their allocated IoT nodes. This network scaling implies increased radio frequency (RF) energy and congestion in the shared wireless channel. Apart from disrupted quality of service, the IoT node is forced to stay in the awake state, continuously monitoring for channel availability, further draining its limited available energy.

We propose to address this spectral congestion by fast-spectrum sensing across a wide spectral band and opportunistically transmitting in the first available spectral band. Furthermore, we propose to opportunistically benefit from efficiently harvesting this increased RF energy from gateway hubs (S_{G1}, S_{G2}) through ($E_{G_1-S_{\mathrm{IoT}}}$, $E_{G_2-S_{\mathrm{IoT}}}$) to enhance/replenish (S_A).

Therefore, we observe that the lifetime of the IoT node depends not only on the nature of its subsystems but also on crucial factors in the design of a robust and reliable energy system due to considerations of systemic interactions, which can either adversely diminish or opportunistically enhance it.

B. Proposed ULP IoT System Architecture

In Table I, we enumerate the key optimizations and corresponding circuit and system implementation. In Fig. 2(b), we present the proposed infrastructure for the ULP IoT system. The information receiver comprises an energy detection-based WuRx and a received signal strength indicator (RSSI) circuit, to perform signal detection and strength characterization. To impart security to the IoT node, we utilize the RSSI circuit to detect an unusual energy pattern in the system and mitigate the EDA. To coexist in the congested network of devices, a spectrum sensor locates the available channel for communication by quickly scanning a wide spectral band. Together with the information receiver, harvesting energy from multiple transmitters in the network enables the IoT radio to also function as an energy receiver. Through a closed-loop beamforming technique, we efficiently harvest the available RF energy in the network.

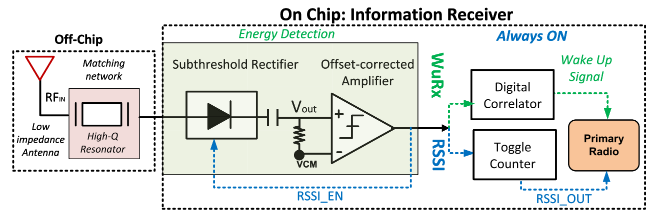

Fig. 3. Proposed information receiver comprises of energy efficient WuRx and RSSI circuit.

III. ULTRA-LOW POWER INFORMATION RECEIVER

A. Received Signal Strength Indicator

In [21], we present the circuit implementation of our RSSI circuit which is one of the first reported methods to combine comparator, rectifier, and digital reset technique to detect the power level of the incoming signal directly into the digital domain. Fig. 3 shows the architecture of our RSSI circuit. The RSSI circuit is implemented in a 65-nm CMOS process with a 1-V supply. Measurement results show that our RSSI circuit achieves a dynamic range of 26 dB, accuracy of ± 0.5 dB, and consumes a power of 6 nW. The measured sensitivity is -55 dBm with a matching network and -38 dBm without it. Our ULP RSSI circuit enables an accurate link assessment of the wireless channel which generally suffers from spatio-temporal fluctuations. In addition to this, it can also be used to monitor RF energy levels in energy harvesting applications, otherwise expensive due to a high power consumption of the conventional RSSI circuit. We also propose a *lightweight* hardware security system to detect and mitigate PHY layer attacks, implemented using our energy efficient RSSI circuit.

B. Wake-Up Radio

System equipped with WuRx can reduce power consumption by activating the primary radio only upon a communication request [22], significantly enabling lower power consumption than currently available radios leveraging the duty-cycling technique. In Fig. 3, we present energy detection-based passive front-end WuRx with an ultra-low power consumption of 10 nW. The proposed WuRx is based on codesign methodology with the RF front-end which comprises a low impedance antenna and an MEMS resonator [23]. In Fig. 4, we show the measurement setup for over-the-air experiment with ≈ 12-feet distance between the transmitter and receiver. We have tabulated the measurement results in Table II.

C. Hardware Security

An adversary in the IoT network can launch a jamming attack where an IoT device is forced to transmit repeatedly. This leads to frequent wake-ups which drains its limited available energy. Energy detection-based mechanism which use RSSI circuit to indicate jamming attacks [24], [25] can consume several milli-watts (mW) of power which overloads the energy limited ULP

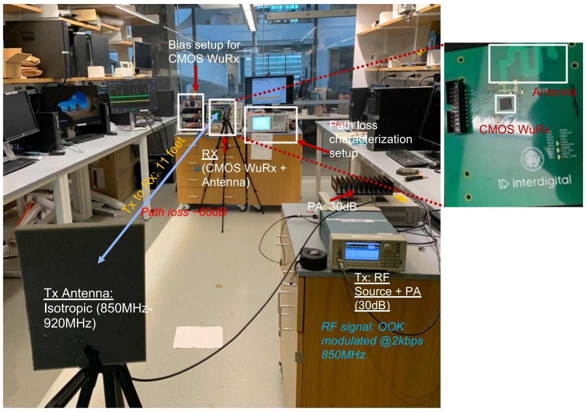

Fig. 4. Wireless setup for characterizing WuRx with RF passive front-end.

TABLE II
MEASUREMENT RESULTS OF WURX WITH PASSIVE FRONT-END

Technology	65nm CMOS
Sensitivity (dBm)	**-60# | -45***
Frequency (MHz)	850
Supply Voltage(V)	1
Data Rate (kbps)	10
Power consumption (nW)	10
Silicon Area (mm^2)	0.04
Bandwidth (GHz)	0.75

#*Measured at* 850 *MHz using off-chip matching network*, **Measured at* 900 *MHz without off-chip matching network*

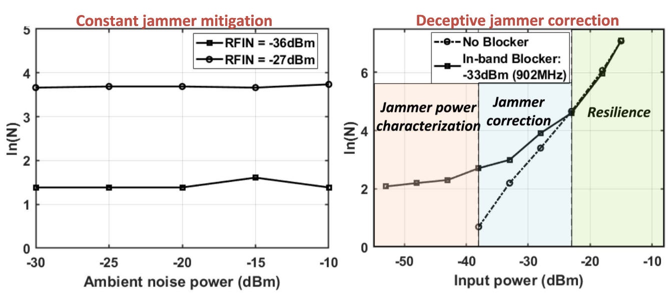

(a) (b)

Fig. 5. Measurement results of our RSSI circuit, to be deployed as a *lightweight* security system to mitigate. (a) Constant jamming attacks. (b) Deceptive/periodic jamming attacks.

IoT system. We extend the application of ULP RSSI circuit discussed in Section III-A as a *lightweight* hardware security solution to mitigate effect of constant and deceptive jamming attacks on the information receiver.

From [21], we note that the output toggle count of the RSSI circuit is given by

$$\ln(N) = \alpha P_{\text{in}} + \beta \tag{1}$$

where P_{in} is the incoming RF signal power, and β is a constant.

Based on (1), we detect anomalies by observing variations in the received signal. The performance of our security solution against specific jamming modalities is discussed as follows.

1) Constant Jamming Attack: Fig. 5(a) shows the measurement result for a constant jammer. Under a constant jamming attack, the rectifier circuit output settles to its corresponding

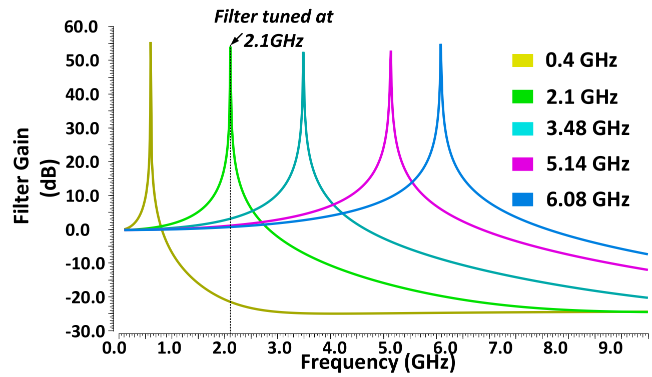

Fig. 6. Simulation results of the proposed narrow-band programmable on-chip spectrum sensor.

dc voltage level which is *filtered* through ac-coupling (Fig. 3). Thus, the proposed RSSI circuit only responds to the primary RF signal and toggle count/*wake-up signal* is unaffected even in the presence of a constant jammer.

2) Deceptive Jamming Attack: Deceptive jammer sends a continuous stream of data bits to deceive the ULP IoT into assuming a legitimate communication-request depriving the desired sleep mode with frequent wake-ups. Fig. 5(b) shows the measurement results of the proposed ULP RSSI circuit under a deceptive jamming attack. In the presence of deceptive jammer, for a low power of primary RF signal, the output toggles are entirely attributed to the deceptive jammer [*jammer power characterization* in Fig. 5(b)]. This toggle count is set as threshold in the digital correlator to prevent frequent wake-up of the primary radio [*jammer correction* in Fig. 5(b)]. At a higher power of the primary RF signal, the toggle count is unaffected because of the increased signal-to-interference ratio (SIR) [*Resilience* in Fig. 5(b)].

D. Spectrum Sensing

Spectrum sensing is crucial for coexistence in congested spectral environments, enabling the detection of RF signals from primary users across a broad RF spectrum. Spectrum sensing techniques reported in literature [26], [27], [28], [29], [30], [31], [32] include sampling of the RF signal using a high-bandwidth analog-to-digital converter (ADC) followed by a digital fast Fourier transform (FFT) block [31]. Energy detection-based techniques measure the power level of RF signal in the band of interest and compare it with expected noise power in the absence of the RF signal [32]. An analog implementation is more suitable for high-frequency applications but accurate sensing of noise level is needed. In Fig. 6, we present the simulation results of a narrow-band, programmable, on-chip filter for spectrum sensing. The on-chip filter performs energy detection in a narrow band around the selected (programmed) frequency. We propose a fast convergence (< 1 μs) spectrum sensing technique to sense (0.4–6 GHz) frequency band for communication. Fast sensing enables the IoT node to quickly identify and utilize available channel for communication with the gateway device. This reduction in waiting time facilitates better coexistence in the shared spectrum and extends battery lifetime. Mittal et al. [33] presented

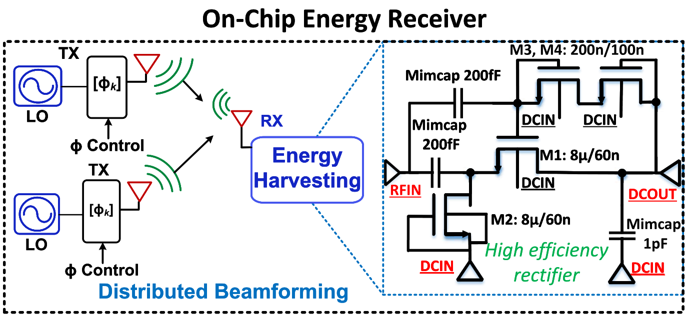

Fig. 7. Proposed energy receiver consists of a high-efficiency rectifier and distributed beamforming technique to boost the IoT node's energy system.

a detailed system-level analysis of agile communication, including simulations that demonstrate agile interactions between IoT nodes and edge devices, enabled by our fast on-chip spectrum sensor.

IV. Energy Receiver

In Fig. 7, we present the energy receiver for the ULP IoT system, comprising a high-efficiency passive RF rectifier and a distributed beamforming technique, to opportunistically harvest an increased level of RF energy from the congested network of IoT devices and gateways.

A. High-Efficiency Rectifier

In Fig. 7, the antenna captures the RF signal and transmits it to the rectifier through a matching network. The rectifier then converts the RF signal into a dc output. The primary challenge in this process is achieving high power conversion efficiency (PCE), which is defined as the ratio of the delivered output dc power to the received RF input power. Given that the input RF signal amplitude is often relatively small, the system requires a low-loss rectifier and an effective matching network. Besides PCE, other crucial parameters such as sensitivity and output dc voltage play a significant role in assessing the system's performance. Sensitivity refers to the minimum input power level needed to achieve the desired output voltage. It evaluates the rectifier performance in the low incident power regime and becomes the bottleneck of the effective wireless energy transfer distance. The peak PCE range is also limited by the nature of typical rectifier topology. Therefore, in this energy detection application, prioritizing sensitivity and PCE range for rectifier design is essential to extend the operation range of the device and increase overall system reliability.

In the initial implementations of threshold compensation methods, the dc output level from subsequent diode stages was utilized to bias the gate of the current half-wave stage [34], [35]. However, as power levels increased, this bias voltage became substantial, resulting in conduction even during the reverse conduction phase. To address this issue, adaptive biasing techniques allow adjustment of biasing requirements based on the input power level [36], [37]. However, these techniques necessitate more intricate biasing structures and a quiescent current for biasing, derived from the output of rectifying stages. A nonlinear biasing technique is essential to adapt biasing in accordance with the input power, ensuring adequate bias for lower power and overcoming the leakage problem at higher power levels. The proposed self-biased gate rectifier topology [38] mitigates the "dead zone" of the Dickson multiplier in low input power by forming a high impedance path to bias the gate of the pumping transistor and also prevents reverse leakage in high input power conditions. Hence, it realizes high-efficiency operation over a wide input power range. The measured peak efficiency is 31% at 1-dBm input power with 100-kΩ load. Aside from the rectifier itself, the power loss in the entire system also results from the reflection loss due to impedance mismatch and quality factor of the matching network. There also exists one optimal load condition for maximum power extraction which is critical for the wireless energy transfer scheme.

B. Distributed Beamforming

Distributed RF beamforming is a promising technique to transfer energy to a remotely located receiver [39], [40], [41], [42], [43], [44], [45]; however, its efficacy depends on how well the transmission phases are aligned at the receiver. Commonly used techniques based on channel state information (CSI) and RSSI have higher power consumption and require baseband signal processing capabilities, which are often not viable in low power, low-cost sensing devices. In Fig. 7, we visualize a closed-loop RF beamforming wireless power transfer scheme using a ULP received-power sensing technique and feedback-based optimization. These techniques can enable closed-loop beamforming with nanowatts power overhead leading to an enhanced energy system for ULP IoT system.

C. Simulation Results

The simulation in Fig. 8(b) illustrates the relationship between received output voltage and time. The simulation results are obtained assuming an optimal beamforming, where phase and frequency offsets are corrected. We assume that the transmit power is 30 dBm for each transmitter, and consider a random distance from 6 to 17 feet between the receivers with transmitting frequency being 915 MHz, as depicted in Fig. 8(a). Fig. 8(b) shows the increasing trend of output voltage at the output of the rectifier while incident powers of -16, -13, -10, and -7 dBm are applied sequentially. These power numbers represent the incident power received by the antenna which will vary with transmitting power, distance, and signal frequency. To evaluate the RF energy harvesting, measurements were conducted using a commercial rectifier. The commercial RF energy harvester (POWERCAST P21XXCSR-EVB) [46] comprises a passive rectifier and a boost converter to regulate the output voltage. In Fig. 8(c), the measurement results of the rectifier's output power with RF signal power sweep are depicted. It is noted that with 2-TX alone, the rectifier can achieve an output power of up to 108 μW with -3-dBm input power. By employing wireless beamforming from m-Tx, the power at the receiver is increased, thereby amplifying the signal energy by a factor of m^2. This enhances the IoT energy system's capability to support ULP IoT applications.

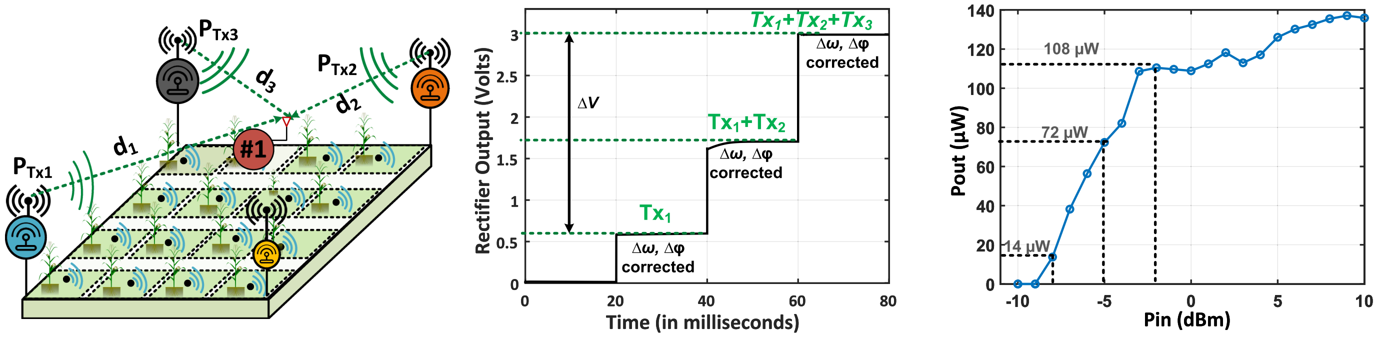

(a) (b) (c)

Fig. 8. (a) Simplified framework for harvesting RF energy from gateway devices installed on an agricultural farm. (b) Simulation results showcasing the increased rectifier output voltage obtained through RF energy harvesting from multiple RF energy transmitters. (c) Measurement results of the output power of a commercial rectifier with input RF power.

TABLE III
Parameter Definition for Energy System Analysis

Parameter	Definition
Sensor Parameters	
$I_{s,\text{on}}$	ON mode current
$I_{s,\text{off}}$	OFF mode current
$T_{s,\text{on}}$	ON time
$T_{s,\text{off}}$	OFF time
Processor Parameters	
$I_{p,\text{on}}$	ON mode current
$I_{p'}$	Infrastructure circuits current
$T_{p,\text{on}}$	ON time
$T_{p,\text{off}}$	OFF time
Radio Parameters	
$I_{r,\text{on}}$	ON mode current
$I_{r,\text{off}}$	OFF mode current
I_{WuRx}	WuRx current
$T_{r,\text{on}}$	ON mode current
$T_{r,\text{off}}$	OFF mode current
Battery Parameters	
B_{cap}	Battery capacity
Spatial Parameters	
A_{farm}	Total farm area
A_{sense}	Sensor spatial resolution

V. Energy System Analysis

We conduct a comprehensive analysis to present the power consumption characteristics of various sensors deployed in precision agriculture. We explore different scenarios involving battery-powered energy systems and investigate the integration of our proposed energy harvesting system, leveraging beamforming technology. The critical parameters utilized in our analysis are detailed in Table III. Initially, we introduce a generic sensing framework, followed by a case study involving commercial sensors to illustrate our analysis.

A. *Sensor Power Consumption Analysis*

We make the following assumptions for our analysis.

1) Each sensor hub incorporates "n" distinct modalities within the sensor domain, encompassing parameters, such as soil temperature, soil porosity, ambient conditions among others [1], [8], [57], [58]. This is visualized in Fig. 9.

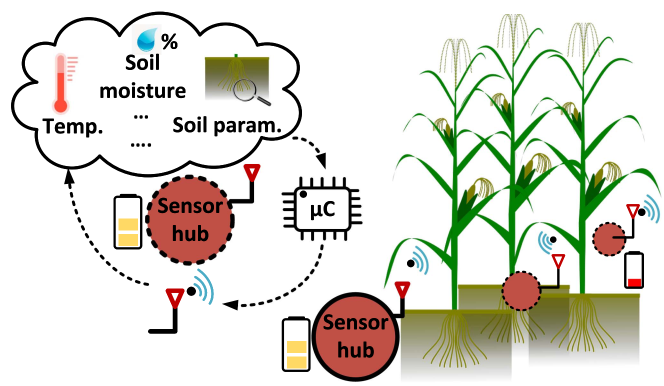

Fig. 9. Battery-powered sensor hub with sensors, processor, and radio for farm parameter monitoring and data transmission to the gateway.

2) Each sensor hub operates with varying duty cycles during T_{hub} (1 d).
3) Each sensor hub is equipped with a single processing unit and radio communication module to facilitate its operations.
4) The WuRx system operates continuously and consumes a current of I_{WuRx}.
5) Each sensor hub is powered by a single battery with a capacity of B_{cap}.

The number of sensor hubs deployed over the farm for sensing and monitoring applications is given by the ratio of total farm area to the spatial resolution of each sensor hub

$$N = \frac{A_{\text{farm}}}{A_{\text{sense}}}. \tag{2}$$

The current consumption of sensors in both active (ON) and leakage (OFF) modes is defined as follows:

$$I_{s,\text{hub}|\text{ on}} = \frac{\sum_{i=1}^{n}\left(I_{s,\text{on}_i} \cdot T_{s,\text{on}_i}\right)}{T_{\text{hub}}} \tag{3}$$

$$I_{s,\text{hub}|\text{ off}} = \frac{\sum_{i=1}^{n}\left(I_{s,\text{off}_i} \cdot T_{s,\text{off}_i}\right)}{T_{\text{hub}}}. \tag{4}$$

Assuming an always-ON infrastructure circuit, the current consumption of the processing system in both active (ON) and leakage (OFF) modes is calculated as

$$I_{p,\text{hub}|\text{ on}} = \frac{(I_{p,\text{on}} \cdot T_{p,\text{on}})}{T_{\text{hub}}} + I_{p'} \tag{5}$$

$$I_{p,\text{hub}|\text{ off}} = \frac{(I_{p,\text{off}} \cdot T_{p,\text{off}})}{T_{\text{hub}}} + I_{p'}. \tag{6}$$

Similarly, the current consumption of the communication system in both active (ON) and leakage (OFF) modes is given by

$$I_{r,\text{hub}|\text{ on}} = \frac{(I_{r,\text{on}} \cdot T_{r,\text{on}})}{T_{\text{hub}}} + I_{\text{WuRx}} \tag{7}$$

$$I_{r,\text{hub}|\text{ off}} = \frac{(I_{r,\text{off}} \cdot T_{r,\text{off}})}{T_{\text{hub}}} + I_{\text{WuRx}}. \tag{8}$$

The total current consumption in both active (ON) and leakage (OFF) modes is the sum of the individual components

$$I_{\text{hub}|\text{ on}} = I_{s,\text{hub}|\text{ on}} + I_{p,\text{hub}|\text{ on}} + I_{r,\text{hub}|\text{ on}} \tag{9}$$

$$I_{\text{hub}|\text{ off}} = I_{s,\text{hub}|\text{ off}} + I_{p,\text{hub}|\text{ off}} + I_{r,\text{hub}|\text{ off}}. \tag{10}$$

The total current consumption of the sensor hub is calculated as

$$I_{\text{hub}|\text{ total}} = I_{\text{hub}|\text{ on}} + I_{\text{hub}|\text{ off}}. \tag{11}$$

B. Battery-Based Energy System

Battery lifetime can be calculated as

$$T_{\text{battery}|\text{days}} = k_{\text{batt}} \cdot \frac{B_{\text{cap}}}{I_{\text{hub}|\text{ total}}} \tag{12}$$

where k_{batt} represents the battery discharge factor. This factor quantifies the reduction in battery performance under specific operational conditions compared to its rated capacity. Influences on this factor include temperature, usage history, and discharge rate, among others [59], [60], [61]. Number of battery replacements for the entire farm after $T_{\text{battery}|\text{days}}$ is given by N from (2). Alongside battery capacity, factors such as form factor and cost are crucial considerations in battery selection.

C. Energy Harvesting Using Beamforming

Consider a wireless distributed beamforming system with m transmitters. Power received at the Rx is [62], [63]

$$P_{Rx,\text{beam}} = m^2 \cdot P'_{Tx} \tag{13}$$

where P'_{Tx} is the effective transmitted power after accounting for wireless path loss.

Subsequently, the rectifier circuit will harness $P_{Rx,\text{beam}}$, converting it into dc power. The output power of the rectifier is determined by

$$P_{\text{harvest}} = P_{Rx,\text{beam}} \cdot \eta_{\text{rect}} \tag{14}$$

where η_{rect} represents the efficiency of the rectifier. For a transmission time slot of T_{slot}, the received energy (E_{harvest} at the rectifier output (assuming no loss) can be obtained as

$$E_{\text{harvest}} = \int_0^{T_{\text{slot}}} P_{\text{harvest}}(t)\, dt. \tag{15}$$

The specific energy requirements for sensor operation determine the selection of signal encoding, transmission timeslot, and receiver architecture for wireless power transfer [63]. Furthermore, simultaneous wireless information and power transfer techniques employ various receiver structures and maximum power point tracking [64] to optimize wireless power delivery.

The current supply capacity of the energy harvesting system is determined by

$$I_{\text{harvest}} = \frac{P_{\text{harvest}}}{V_{\text{dc}}} \cdot k_{\text{reg}}. \tag{16}$$

Here, k_{reg} factors in the losses incurred during voltage conversion performed by dc–dc converters.

There are two modalities in which this harvested energy can be utilized for system operation: 1) direct energy transfer using the harvest-use architecture or 2) utilizing stored energy with the harvest-store-use architecture [39].

1) Harvest-Use: In the harvest-use architecture, the harvested energy is directly utilized for system operation. To enhance reliability, the current requirement should not exceed the energy harvesting capability, meaning that $I_{\text{harvest}} \geq I_{\text{hub}}$.

2) Harvest-Store-Use: In the harvest-store-use architecture, energy harvested is commonly stored in a storage capacitor, such as supercapacitors or rechargeable batteries, guaranteeing a consistent energy supply to the system. It is essential to carefully determine the dimensions of the supercapacitor and minimize discharge to achieve optimal energy management [65], [66].

Considering a simple *RC* circuit, the equivalent resistor to calculate the discharge time of the capacitor, accounting for system current consumption, is determined by

$$R_{\text{eq}} = \frac{V_{\text{supply}}}{k_{\text{disc}} \cdot I_{\text{hub}|\text{ total}}} \tag{17}$$

where k_{disc} accounts for the self-discharge of the supercapacitor. Therefore, for a supercapacitor of capacitor value of C, the discharge time is given by [67]

$$t_{\text{discharge}} = -R_{\text{eq}} \cdot C \cdot \log\left(\frac{V_{\text{supply}}}{V_{\text{min}}}\right) \tag{18}$$

where V_{min} represents the minimum operating voltage which is less than V_{supply}.

It is important to ensure that the supercapacitor is sized appropriately so that, even during periods of peak current consumption, the voltage remains above V_{min}.

D. Case Study of a Practical System

To assess the system and evaluate the viability of various energy systems, we have analyzed a sensor hub, which monitors agricultural farm conditions, processes the gathered data, and transmits it to a gateway device. The sensor modalities include soil temperature, soil moisture, ambient humidity, and light

TABLE IV
CASE STUDY OF A SENSOR HUB DEPLOYED FOR SENSING AND MONITORING ON AN AGRICULTURAL FARM

Component	Product	Active current (mA)	Leakage current (mA)	Average Current (mA)
Sensing				
Soil Temperature	THERM200 [47]	13	3.00E-04	3.31E-03
Soil Moisture	VH400 [48]	3	0.00E+00	6.94E-04
Relative Humidity	VG-HUMID [49]	2	3.00E-04	7.63E-04
Luminosity	LT150 [50]	3	0.00E+00	6.94E-04
Sensor average current (mA)				***4.77E-03***
Processing				
Microcontroller	C8051F99x [51]	0.075	0.0003	3.03E-04
Infrastructure circuits*	TLF35584QKVS1 [52]	1.00E-01	1.00E-03	1.00E-03
Processor average current (mA)				***1.31E-03***
Communication				
Radio	WLR089U0 [53]	128	0.001608	3.98E-03
WuRx	[21]	6.00E-6	6.00E-6	6.00E-6
Radio average current (mA)				***3.98E-03***
Sensor hub average current (mA)				***1.51E-02***
Battery				
Batteries		**Battery Capacity (mAh)****	**Battery lifetime (months)**	
Serial LIR2032 [54]		70	5.2	
Duracell 2032 [55]		230	16.9	
Eagle Pitcher [56]		350	25.8	

* Estimated power consumption, ** considering rated capacity.

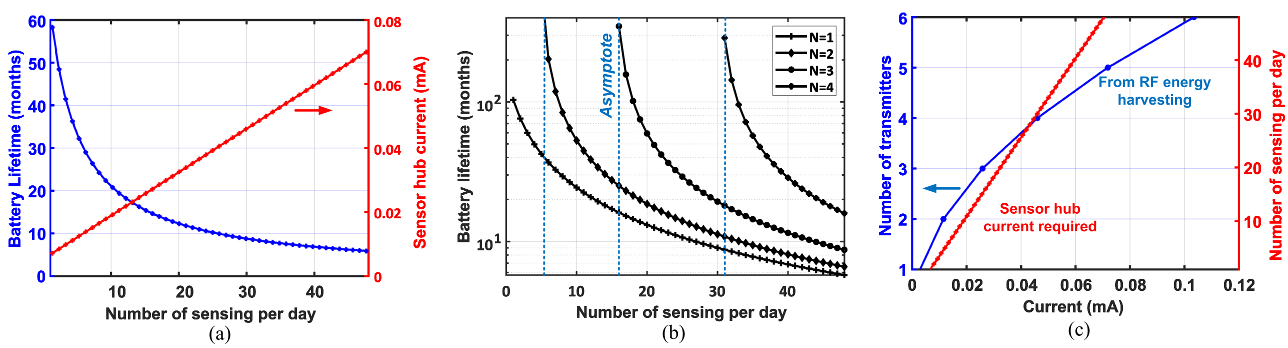

Fig. 10. (a) Decrease in battery lifetime with increased temporal resolution of sensing and monitoring. (b) Enhanced battery lifetime with energy augmentation from energy harvesting for varying number of transmitters. (c) Feasibility of energy harvesting for a self-powered IoT system.

intensity. A microcontroller processes the sensed information, with additional infrastructure circuits, such as power management and timing circuits included in the processing system [9]. The communication setup consists of a primary radio and a WuRx unit.

We have computed the power consumption of each design component to evaluate battery lifespan and explore the potential for utilizing energy harvesting to sustain the system. The sensor hub operates on a duty cycle, ensures sensor data stability, and has an active time for the sensors set to 2.5 s. The processor operates with an active time of 500 ms. The primary radio transmits at 1 KHz sending 200 bits and stays in active mode for 200 ms. We have conducted battery life calculations for various batteries, opting for low-cost and compact options for our analysis. The data are presented for eight sensing instances per day. We have provided approximate numbers; however, the crucial aspect lies not in the precise accuracy of these numbers but rather in selecting the appropriate energy system based on these estimations.

Using the data from Table IV, we investigate three distinct scenarios regarding the selection of energy systems to power the IoT sensor hub. The detailed analyses conducted are showcased in Fig. 10. These scenarios are elaborated as follows.

1) Battery-Based Energy System: We conducted analysis to evaluate battery lifespan, varying the frequency of sensing operations per day. The analysis outcomes are depicted in Fig. 10(a), illustrating both battery lifespan and current consumption against the number of daily sensing readings. It is observed that with a sensing frequency of every 30 min per day, the battery lifespan for a battery with a capacity of 350 mAh is reduced to 5.5 mo.

To understand the implications of battery replacements for agricultural operations, let us consider a farm covering an area of 1 acre (43560 sq. ft.), with each sensor hub deployed in a 25 sq. ft. area. This indicates a requirement for 1742 sensor hubs to cover the entire field. Consequently, if sensing is performed every 30 min per day, an average of 1742 battery replacements would be necessary every 5.5 mo. Such frequent replacements are highly inconvenient and pose a challenge to our objective of establishing a "deploy and forget" IoT system.

2) Hybrid Battery and Energy Harvesting System: In this scenario, we have integrated energy harvesting alongside the

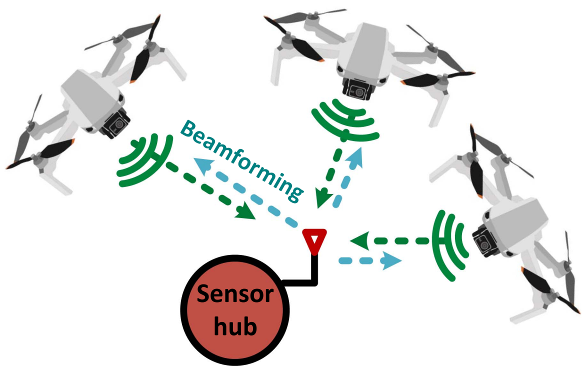

Fig. 11. Envisioned future of wireless charging utilizing drones.

battery-based system, thereby enhancing the capabilities of the existing setup. Fig. 10(b) depicts the analysis results obtained by harvesting RF energy from varying numbers of RF transmitters. In our configuration, each transmitter emits at 25 dBm and experiences a path loss of 40 dB for a distance of 2.5 m at a frequency of 915 MHz. It is evident that by utilizing distributed wireless power from multiple transmitters, the battery lifespan is significantly improved. The curve approaching an asymptote suggests that the energy harvesting current can adequately meet the current requirements of the sensor hub, thus obviating the need for a battery. For scenarios involving more than four transmitters, as specified in the power consumption details of the sensor hub in Table IV, the need for a battery is completely eliminated.

3) Energy Harvesting Only: Fig. 10(c) illustrates the scenario where only energy harvesting powers the sensor hub. We utilized the transmitter setup from the previous case. It is evident that the energy harvesting can meet the sensor hub's current requirement based on the number of sensing operations per day, especially when utilizing more than four transmitters (crossover point). By employing more than four transmitters, the harvested current capacity exceeds the sensor hub's current needs. In addition, the surplus energy availability enables an expansion in both sensing modalities and temporal resolution for precision agriculture.

Moreover, a detailed quantitative analysis is essential for a comprehensive assessment of the efficacy of RF energy harvesting. This analysis would not only provide deeper insights into wireless harvesting system design but also address the impact of environmental factors. These include spatio-temporal channel dynamics, atmospheric conditions (weather and temperature), physical obstructions, and signal interference, all of which significantly affect the efficiency of RF energy harvesting. Each factor should be meticulously evaluated to enhance understanding and optimization of system performance [68], [69], [70], [71].

E. Future Wireless Charging

By leveraging distributed beamforming alongside frequency and phase offset corrections, as outlined in [72], a conceptualized fly-by wireless power transfer system employing multiple drones could be realized. In this scenario, each drone would initially enter a designated receiver operational range and commence self-charging from ambient transceivers or other drones by adjusting phase and frequency offsets. The visualization of this process is depicted in Fig. 11. These drones, capable of remaining in motion, present a practical approach to achieve an efficient wireless power transfer.

VI. Conclusion

This article presented an energy-efficient, secure, and spectrum-aware infrastructure for the ULP IoT system to support sensing and monitoring for precision agriculture. We introduced a system graph model and identified critical optimizations for the ULP IoT system. We presented measurement results of energy detection-based infrastructural blocks (WuRx and RSSI) which improve energy efficiency and security of the IoT system. We proposed a fast-scanning spectrum sensor for better spectrum coexistence, and discussed an energy receiver topology that can potentially enable IoT system to be driven by the harvested energy leading to self-powered system. In addition, we conducted a detailed analysis of the sensor hub's power consumption through a practical case study, evaluating the potential of energy harvesting to achieve energy autonomy in precision agriculture sensing and monitoring.

In future endeavors, a promising direction would be to conduct a thorough assessment and implementation of RF energy harvesting utilizing distributed beamforming, taking into account critical environmental factors such as spatio-temporal channel dynamics, atmospheric conditions, physical barriers, and signal interference, all of which significantly influence harvesting efficiency. In addition, developing innovative security methodologies by exploring more complex jamming scenarios within IoT networks can enhance the proposed *lightweight* security solutions. To further advance precision agriculture, the integration of emerging technologies, such as artificial intelligence, blockchain analytics, and agricultural robotics could broaden the scope and impact of IoT sensing and monitoring.

References

[1] M. S. Farooq, S. Riaz, A. Abid, K. Abid, and M. A. Naeem, "A survey on the role of IoT in agriculture for the implementation of smart farming," *IEEE Access*, vol. 7, pp. 156237–156271, 2019.

[2] Y. Chen and Y. Li, "Intelligent autonomous pollination for future farming—A micro air vehicle conceptual framework with artificial intelligence and human-in-the-loop," *IEEE Access*, vol. 7, pp. 119706–119717, 2019.

[3] N. Ahmed, D. De, and I. Hussain, "Internet of things (IoT) for smart precision agriculture and farming in rural areas," *IEEE Internet Things J.*, vol. 5, no. 6, pp. 4890–4899, Dec. 2018.

[4] R. K. Singh, R. Berkvens, and M. Weyn, "AgriFusion: An architecture for IoT and emerging technologies based on a precision agriculture survey," *IEEE Access*, vol. 9, pp. 136253–136283, 2021.

[5] M. Ayaz, M. Ammad-Uddin, Z. Sharif, A. Mansour, and E.-H. M. Aggoune, "Internet-of-things (IoT)-based smart agriculture: Toward making the fields talk," *IEEE Access*, vol. 7, pp. 129551–129583, 2019.

[6] P. Anand, Y. Singh, A. Selwal, M. Alazab, S. Tanwar, and N. Kumar, "IoT vulnerability assessment for sustainable computing: Threats, current solutions, and open challenges," *IEEE Access*, vol. 8, pp. 168825–168853, 2020.

[7] S. Qazi, B. A. Khawaja, and Q. U. Farooq, "IoT-equipped and AI-enabled next generation smart agriculture: A. critical review, current challenges and future trends," *IEEE Access*, vol. 10, pp. 21219–21235, 2022.

[8] V. P. Kour and S. Arora, "Recent developments of the Internet of Things in agriculture: A survey," *IEEE Access*, vol. 8, pp. 129924–129957, 2020.
[9] N. Shafiee, S. Tewari, B. Calhoun, and A. Shrivastava, "Infrastructure circuits for lifetime improvement of ultra-low power IoT devices," *IEEE Trans. Circuits Syst. I: Regular Papers*, vol. 64, no. 9, pp. 2598–2610, Sep. 2017.
[10] M. N. Mowla, N. Mowla, A. F. M. S. Shah, K. M. Rabie, and T. Shongwe, "Internet of Things and wireless sensor networks for smart agriculture applications: A survey," *IEEE Access*, vol. 11, pp. 145813–145852, 2023.
[11] D. Glaroudis, A. Iossifides, and P. Chatzimisios, "Survey, comparison and research challenges of IoT application protocols for smart farming," *Comput. Netw.*, vol. 168, Feb. 2020, Art. no. 107037, doi: 10.1016/j.comnet.2019.107037.
[12] A. Yazdinejad et al., "A review on security of smart farming and precision agriculture: Security aspects, attacks, threats and countermeasure," *Appl. Sci.*, vol. 11, no. 16, 2021, Art. no. 7518.
[13] U. Shafi, R. Mumtaz, J. García-Nieto, S. A. Hassan, S. A. R. Zaidi, and N. Iqbal, "Precision agriculture techniques and practices: From considerations to application," *Sensors*, vol. 19, no. 17, 2019, Art. no. 3796.
[14] M. S. Farooq, S. Riaz, A. Abid, T. Umer, and Y. B. Zikria, "Role of IoT technology in agriculture: A systematic literature review," *Electronics*, vol. 9, no. 2, 2020, Art. no. 319.
[15] M. Gupta, M. Abdelsalam, S. Khorsandroo, and S. Mittal, "Security and privacy in smart farming: Challenges and opportunities," *IEEE Access*, vol. 8, pp. 34564–34584, 2020.
[16] A. Mittal and A. Shrivastava, "Detecting continuous jamming attack using ultra-low power RSSI circuit," in *Proc. IEEE Int. Symp. Hardware Oriented Secur. Trust*, 2022, pp. 49–52.
[17] D. Alghazzawi, O. Bamasaq, S. Bhatia, A. Kumar, P. Dadheech, and A. Albeshri, "Congestion control in cognitive IoT-based WSN network for smart agriculture," *IEEE Access*, vol. 9, pp. 151401–151420, 2021.
[18] M. Jamshidi, *Systems of Systems Engineering: Principles and Applications*. Boca Raton, FL, USA: CRC Press, 2009.
[19] P. S. Satsangi and J. B. Ellis, "A generalized system-theoretic framework for modelling large scale national economic systems in dynamic, structural and spatial terms," *Int. J. Syst. Sci.*, vol. 2, pp. 213–223, 1971.
[20] P. S. Satsangi, "A physical system theory modeling framework for transportation system studies," *IEEE Trans. Syst., Man, Cybern.*, vol. 7, no. 11, pp. 763–778, Nov. 1977.
[21] A. Mittal et al., "A ±0.5 dB, 6 nW RSSI circuit with RF power-to-digital conversion technique for ultra-low power IoT radio applications," *IEEE Trans. Circuits Syst. I: Regular Papers*, vol. 69, no. 9, pp. 3526–3539, Sep. 2022.
[22] R. Piyare, A. L. Murphy, C. Kiraly, P. Tosato, and D. Brunelli, "Ultra low power wake-up radios: A. hardware and networking survey," *IEEE Commun. Surv. Tut.*, vol. 19, no. 4, pp. 2117–2157, Fourthquarter 2017.
[23] G. Michetti et al., "Hybridly integrated MEMS-IC RF front-end for IoT with embedded filtering and passive voltage amplification," in *Proc. IEEE Sensors Conf.*, 2021, pp. 1–4.
[24] W. Xu, W. Trappe, Y. Zhang, and T. Wood, "The feasibility of launching and detecting jamming attacks in wireless networks," in *Proc. 6th ACM Int. Symp. Mobile ad hoc Netw. Comput.*, New York, NY, USA, 2005, pp. 46–57, doi: 10.1145/1062689.1062697.
[25] A. D. Wood, J. A. Stankovic, and G. Zhou, "DEEJAM: Defeating energy-efficient jamming in IEEE 802.15.4-based wireless networks," in *Proc. 4th Annu. IEEE Commun. Soc. Conf. Sensor, Mesh Ad Hoc Commun. Netw.*, 2007, pp. 60–69.
[26] D. Cabric, S. Mishra, and R. Brodersen, "Implementation issues in spectrum sensing for cognitive radios," in *Proc. Conf. Rec. 38th Asilomar Conf. Signals, Syst. Comput.*, 2004, pp. 772–776.
[27] N.-S. Kim and J. M. Rabaey, "A high data-rate energy-efficient triple-channel UWB-based cognitive radio," *IEEE J. Solid-State Circuits*, vol. 51, no. 4, pp. 809–820, Apr. 2016.
[28] A. Ghasemi and E. S. Sousa, "Spectrum sensing in cognitive radio networks: Requirements, challenges and design trade-offs," *IEEE Commun. Mag.*, vol. 46, no. 4, pp. 32–39, Apr. 2008.
[29] J. Park et al., "A fully integrated UHF-Band CMOS receiver with multi-resolution spectrum sensing (MRSS) functionality for IEEE 802.22 cognitive radio applications," *IEEE J. Solid-State Circuits*, vol. 44, no. 1, pp. 258–268, Jan. 2009.
[30] K. Banović and T. C. Carusone, "A sub-mw spectrum sensing architecture for portable IEEE 802.22 cognitive radio applications," in *Proc. IEEE Int. Symp. Circuits Syst.*, 2017, pp. 1–4.
[31] D. Cabric, A. Tkachenko, and R. W. Brodersen, "Experimental study of spectrum sensing based on energy detection and network cooperation," in *Proc. 1st Int. Workshop Technol. Policy Accessing Spectr.*, New York, NY, USA, 2006, pp. 12–es, doi: 10.1145/1234388.1234400.
[32] H. Urkowitz, "Energy detection of unknown deterministic signals," *Proc. IEEE*, vol. 55, no. 4, pp. 523–531, Apr. 1967, doi: 10.1109/PROC.1967.5573.
[33] A. Mittal et al., "Sub-6 GHz energy detection-based fast on-chip analog spectrum sensing with learning-driven signal classification," *IEEE Internet Things J.*, to be published, doi: 10.1109/JIOT.2024.3392428.
[34] J. F. Dickson, "Voltage multiplier employing clock gated transistor chain" U.S. Patent US4214174A, Jul. 1980.
[35] G. Papotto, F. Carrara, and G. Palmisano, "A 90-nm CMOS threshold-compensated RF energy harvester," *IEEE J. Solid-State Circuits*, vol. 46, no. 9, pp. 1985–1997, Sep. 2011.
[36] Z. Hameed and K. Moez, "A 3.2 V. –15 dBm adaptive threshold-voltage compensated RF energy harvester in 130 nm CMOS," *IEEE Trans. Circuits Syst. I: Regular Papers*, vol. 62, no. 4, pp. 948–956, Apr. 2015.
[37] P. Saffari, A. Basaligheh, and K. Moez, "An RF-to-DC rectifier with high efficiency over wide input power range for RF energy harvesting applications," *IEEE Trans. Circuits Syst. I: Regular Papers*, vol. 66, no. 12, pp. 4862–4875, Dec. 2019.
[38] Z. Xu et al., "A 30% efficient high-output voltage fully integrated self-biased gate RF rectifier topology for neural implants," *IEEE J. Solid-State Circuits*, vol. 57, no. 11, pp. 3324–3335, Nov. 2022.
[39] X. Lu, P. Wang, D. Niyato, D. Kim, and Z. Han, "Wireless networks with RF energy harvesting: A contemporary survey," *IEEE Commun. Surv. Tut.*, vol. 17, no. 2, pp. 757–789, Secondquarter 2015.
[40] S. Timotheou, I. Krikidis, G. Zheng, and B. Ottersten, "Beamforming for MISO interference channels with QoS and RF energy transfer," *IEEE Trans. Wireless Commun.*, vol. 13, no. 5, pp. 2646–2658, May 2014.
[41] Y. Zeng and R. Zhang, "Optimized training design for wireless energy transfer," *IEEE Trans. Commun.*, vol. 63, no. 2, pp. 536–550, Feb. 2015.
[42] X. Chen, C. Yuen, and Z. Zhang, "Wireless energy and information transfer tradeoff for limited-feedback multiantenna systems with energy beamforming," *IEEE Trans. Veh. Technol.*, vol. 63, no. 1, pp. 407–412, Jan. 2014.
[43] J. Xu and R. Zhang, "Energy beamforming with one-bit feedback," *IEEE Trans. Signal Process.*, vol. 62, no. 20, pp. 5370–5381, Oct. 2014.
[44] S. Kashyap, E. Björnson, and E. G. Larsson, "On the feasibility of wireless energy transfer using massive antenna arrays in Rician channels," in *Proc. IEEE 16th Int. Workshop Signal Process. Adv. Wireless Commun.*, 2015, pp. 46–50.
[45] R. Zhang and C. K. Ho, "MIMO broadcasting for simultaneous wireless information and power transfer," *IEEE Trans. Wireless Commun.*, vol. 12, no. 5, pp. 1989–2001, May 2013.
[46] Powercast, "P21XXCSR-EVB, Datasheet," 2018. [Online]. Available: https://www.mouser.com/datasheet/2/329/P21XXCSR_EVB_Datasheet_v2_1_1-3159484.pdf
[47] Vege tronix, "THERM200 product page," Accessed: Feb. 12, 2024. [Online]. Available: https://www.vegetronix.com/Products/THERM200/
[48] Vegetronix, "Soil moisture sensor product page," Accessed: Feb. 12, 2024. [Online]. Available: https://vegetronix.com/soil-moisture-sensor
[49] Vegetroni X, "VG-HUMID product page," Accessed: Feb. 12, 2024. [Online]. Available: https://www.vegetronix.com/Products/VG-HUMID/
[50] Ve getronix, "LT150 Product Page," Accessed: Feb. 12, 2024. [Online]. Available: https://www.vegetronix.com/Products/LT150/
[51] Silicon Labs, "C8051f99x data sheet," Accessed: Feb. 12, 2024. [Online]. Available: https://www.silabs.com/documents/public/data-sheets/C8051F99x.pdf
[52] Infineon Technologies, "TLF35584QKVS1 product page," Accessed: Feb. 12, 2024. [Online]. Available: https://www.infineon.com/cms/en/product/power/power-management-ics-pmic-system-basis-chips-sbc/power-management-ics-pmic/optireg-pmic-automotive/tlf35584qkvs1/
[53] Microchip Technology, "Microchip product data sheet," [Online]. Available: https://www.microchip.com/en-us/product/wlr089u0, accessed: Feb. 12, 2024.
[54] Amazon, "LIR2032 rechargeable batteries," Accessed: Feb. 12, 2024. [Online]. Available: https://www.amazon.com/LIR2032-Rechargeable-Batteries-Capacity-Replacement/dp/B0836DQKFC
[55] Duracell, "Cr2032 lithium coin button battery," Accessed: Feb. 12, 2024. [Online]. Available: https://www.duracell.com/en-us/product/cr-2032-lithium-coin-button-battery/

[56] EaglePicher Technologies, "LTC3PN datasheet," Accessed: Feb. 12, 2024. [Online]. Available: https://www.eaglepicher.com/sites/default/files/ltc3pn-0.pdf

[57] J. J. Estrada-López, A. A. Castillo-Atoche, J. Vázquez-Castillo, and E. Sánchez-Sinencio, "Smart soil parameters estimation system using an autonomous wireless sensor network with dynamic power management strategy," *IEEE Sensors J.*, vol. 18, no. 21, pp. 8913–8923, Nov. 2018.

[58] F. K. Shaikh, S. Karim, S. Zeadally, and J. Nebhen, "Recent trends in Internet-of-Things-enabled sensor technologies for smart agriculture," *IEEE Internet Things J.*, vol. 9, no. 23, pp. 23583–23598, Dec. 2022.

[59] X. Tan et al., "Real-time state-of-health estimation of lithium-ion batteries based on the equivalent internal resistance," *IEEE Access*, vol. 8, pp. 56811–56822, 2020.

[60] J. Zhang, S. Ci, H. Sharif, and M. Alahmad, "Real-time state-of-health estimation of lithium-ion batteries based on the equivalent internal resistance," *IEEE Trans. Energy Convers.*, vol. 25, no. 4, pp. 1133–1141, 2010.

[61] R. R. Kumar, C. Bharatiraja, K. Udhayakumar, S. Devakirubakaran, K. S. Sekar, and L. Mihet-Popa, "Advances in batteries, battery modeling, battery management system, battery thermal management, SOC, SOH, and charge/discharge characteristics in EV applications," *IEEE Access*, vol. 11, pp. 105761–105809, 2023.

[62] M. Wentz and K. Chowdhury, "Intra-network synchronization and retrodirective distributed transmit beamforming with UAVs," *IEEE Trans. Veh. Technol.*, vol. 73, no. 2, pp. 2017–2031, Feb. 2024.

[63] S. Bi, C. K. Ho, and R. Zhang, "Wireless powered communication: Opportunities and challenges," *IEEE Commun. Mag.*, vol. 53, no. 4, pp. 117–125, Apr. 2015.

[64] P. Xu, D. Flandre, and D. Bol, "Analysis, modeling, and design of a 2.45-GHz RF energy harvester for SWIPT IoT smart sensors," *IEEE J. Solid-State Circuits*, vol. 54, no. 10, pp. 2717–2729, Oct. 2019.

[65] J. Elizalde, C. Cruces, M. S. Sandoval, X. Eguiluz, and I. Val, "Self-powered photovoltaic Bluetooth low energy temperature sensor node," *IEEE Access*, vol. 9, pp. 111305–111314, 2021.

[66] X. Yue et al., "Development of an indoor photovoltaic energy harvesting module for autonomous sensors in building air quality applications," *IEEE Internet Things J.*, vol. 4, no. 6, pp. 2092–2103, Dec. 2017.

[67] Circuits.dk, "Capacitor discharge calculator," Accessed: Feb. 12, 2024. [Online]. Availble: https://www.circuits.dk/calculator_capacitor_discharge.htm

[68] M. H. Alsharif, S. Kim, and N. Kuruoğlu, "Energy harvesting techniques for wireless sensor networks/radio-frequency identification: A review," *Symmetry*, vol. 11, no. 7, 2019, Art. no. 865.

[69] M. A. Ullah, R. Keshavarz, M. Abolhasan, J. Lipman, K. P. Esselle, and N. Shariati, "A review on antenna technologies for ambient RF energy harvesting andwireless power transfer: Designs, challenges, and applications," *IEEE Access*, vol. 10, pp. 17231–17267, 2022.

[70] Y. Luo, L. Pu, and L. Lei, "Impact of varying radio power density on wireless communications of RF energy harvesting systems," *IEEE Trans. Commun.*, vol. 69, no. 3, pp. 1960–1974, Mar. 2021.

[71] H. H. R. Sherazi, D. Zorbas, and B. O'Flynn, "A comprehensive survey on RF energy harvesting: Applications and performance determinants," *Sensors*, vol. 22, no. 8, 2022, Art. no. 2990. [Online]. Available: https://www.mdpi.com/1424-8220/22/8/2990

[72] A. Shrivastava, "Beamforming wireless power transfer scheme," Patent US20230026315A1, Jan. 26, 2023, Accessed: Feb. 12, 2024. [Online]. Available: https://patents.google.com/patent/US20230026315A1/en

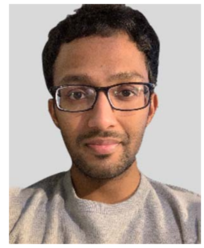

Ankit Mittal (Graduate Student Member, IEEE) received the B.Tech. degree in electronics and communication engineering from Dayalbagh Educational Institute, Agra, India, in 2014. He is currently working toward the Ph.D. degree with the Energy Efficient Circuits and Systems Group, Electrical Engineering, Northeastern University, Boston, MA, USA.

He was a Senior Design Engineer with NXP Semiconductors, Bengaluru, India, with a rich experience in SoC design and five memory testchip tapeout to his credit. His research interests include power management integrated circuit design, ultra-low power biomedical circuits, ultra-low power RF radio design.

Mr. Mittal was the recipient of the 2024 College of Engineering Outstanding Graduate Research Award at Northeastern University. He was also the recipient of Director's medal (Valedictorian Honor) from Dayalbagh Educational Institute.

Ziyue Xu (Graduate Student Member, IEEE) received the B.S. degrees in electrical engineering from Anhui University, Hefei, China, in 2016, and the Ph.D. degree in electrical engineering from Northeastern University, Boston, MA, USA, in 2023.

He is currently a Staff Electrical Engineer with the mobile solutions team, Skyworks Solutions, Inc., Andover, MA, USA. His research interests include power management integrated circuits design, RF design, and energy harvester design.

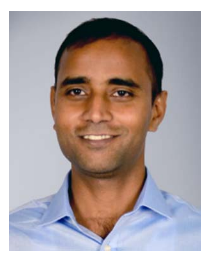

Aatmesh Shrivastava (Senior Member, IEEE) received the Ph.D. degree in electrical engineering from the University of Virginia, Charlottesville, VA, USA, in 2014 .

He was a Senior Design Engineer with Texas Instruments, Bangalore, Karnataka, India, from 2006 to 2010. From 2014 to 2016, he was a Senior Design Director with an IoT start-up Everactive, where he was responsible for the research and development of the energy harvesting and power management solutions. In 2016, he joined Northeastern University, Boston, MA, USA, where he is now working as an Associate Professor with the Electrical and Computer Engineering Department. His research interests include self-powered and ultra-low power circuits and system, energy-harvesting and power-first system/computer architecture, analog computing, Internet-of-Things, ultra-low power bio-medical and neural circuits, exa-scale computing, and hardware security.

Dr. Shrivastava was the recipient of DARPA Young Faculty Award in 2023, NSF CAREER Award in 2022, Acorn Innovation Award from Mass Ventures in 2021, and the 2024 Faculty Fellow Award from the College of Engineering at Northeastern University. He currently serves as an Associate Editor on the editorial board of IEEE Transactions on Circuits and Systems Part I: Regular Papers, IEEE Open Journal on Circuits and Systems, and as a Senior Editor for IEEE Journal on Emerging and Selected Topics in Circuits and Systems.